AD-A270 217

N PAGE

Public r
gather
collectic
Davis H

hour per response, including the time for reviewing instructions, searching existing data sources, action of information. Send comments regarding this burden estimate of any other aspect of this nation headquarters Services, Directorate for Information Operations and Reports, 1215 Jefferson ment and Budget. Paperwork Reduction Project (0704-0188), Washington, DC 03

1. AGENCY USE ONLY (Leave blank)	2. REPORT DATE 8/31/93	3. REPORT TYPE AND DATES COVERED Interim Technical Report 8/1/92–7/31/93

4. TITLE AND SUBTITLE	5. FUNDING NUMBERS
ANISOTROPIC THIRD-ORDER SUSCEPTIBILITY OF A NEMATIC SOLUTION OF A RODLIKE POLYMER (PBT)	
6. AUTHOR(S) HEDI MATTOUSSI and GUY C. BERRY	62102F 2419 00

7. PERFORMING ORGANIZATION NAME(S) AND ADDRESS(ES)	8. PERFORMING ORGANIZATION REPORT NUMBER
Carnegie-Mellon University 5000 Forbes Avenue Pittsburgh, PA 15213-3890	AFOSR-TR· 9 06

9. SPONSORING/MONITORING AGENCY NAME(S) AND ADDRESS(ES)	10. SPONSORING/MONITORING AGENCY REPORT NUMBER
AFOSR/NC Building 410, Bolling AFB DC 20332-6448	F49620-92-J-0281

DTIC
ELECTE
OCT 06 1993
S E D

11. SUPPLEMENTARY NOTES

12a. DISTRIBUTION/AVAILABILITY STATEMENT

APPROVED FOR PUBLIC RELEASE; DISTRIBUTION IS UNLIMITED.

13. ABSTRACT (Maximum 200 words)

Abstract The anisotropic third-order nonlinear optical susceptibility $\chi^{(3)}$ of monodomain samples of nematic solutions of poly[1,4-phenylene-2,6-benzobisthiazole], PBT, a rodlike polymer, have been studied by third harmonic generation. The principal component of $\chi^{(3)}$ $(-3\omega;\omega,\omega,\omega)$ is not along the nematic director, as opposed to the linear dielectric, which has the maximum refractive index along the director.

93-23143

14. SUBJECT TERM	15. NUMBER OF PAGES
	16. PRICE CODE

17. SECURITY CLASSIFICATION OF REPORT	18. SECURITY CLASSIFICATION OF THIS PAGE	19. SECURITY CLASSIFICATION OF ABSTRACT	20. LIMITATION OF ABSTRACT
UNCLASSIFIED	UNCLASSIFIED	UNCLASSIFIED	

ANISOTROPIC THIRD-ORDER SUSCEPTIBILITY OF A NEMATIC SOLUTION OF A RODLIKE POLYMER (PBT)

HEDI MATTOUSSI and GUY C. BERRY

Carnegie Mellon University, Pittsburgh, PA 15213, USA

Abstract The anisotropic third-order nonlinear optical susceptibility $\chi^{(3)}$ of monodomain samples of nematic solutions of poly[1,4-phenylene-2,6-benzobisthiazole], PBT, a rodlike polymer, have been studied by third harmonic generation. The principal component of $\chi^{(3)}(-3\omega;\omega,\omega,\omega)$ is not along the nematic director, as opposed to the linear dielectric, which has the maximum refractive index along the director.

INTRODUCTION

Nonlinear optical properties of organic materials have been of intense interest for the past decade and more, e.g., see references 1-8. The susceptibilities $\chi^{(n)}(-\omega; \omega_1,\omega_2,....\omega_n)$ are macroscopic properties; their relation to molecular characteristics is discussed below. In the dipole approximation, the macroscopic polarization $P(\omega)$ of a material under the influence of an applied fields $E(\omega_1)$, $E(\omega_2)$, etc., propagating with frequencies ω_1, ω_2, etc. (e.g., optical radiation) may be expressed in Cartesian coordinates as:[1-8]

$$P_i(\omega) = \epsilon_0[\chi_{ij}^{(1)} E_j + \chi_{ijk}^{(2)} E_j E_k + \chi_{ijkl}^{(3)} E_j E_k E_l + ...]$$ (1)

where $\omega = \omega_1 + \omega_2 + \omega_3$, etc.; the component notation in Eqn. (1), in which the dependence on frequency is suppressed for convenience, will be used below. In this study, we report measurements of

$\chi^{(3)}(-3\omega;\omega,\omega,\omega)$ by third-harmonic generation on a fully aligned nematic solution of the rodlike polymer poly[1,4-phenylene-2,6-benzobisthiazole], PBT
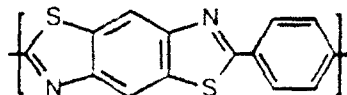
PBT

The polymer is dissolved in a strong protic acid and is, therefore, protonated.[9] Prior measurements of $\chi^{(3)}(-3\omega;\omega,\omega,\omega)$ have been for isotropic solutions of PBT in the same solvent and on PBT dispersed in an organic matrix.[10,11] In addition, $\chi^{(3)}(-3\omega;\omega,\omega,\omega)$ and $\chi^{(3)}(-\omega;\omega,-\omega,\omega)$ have been studied for undiluted PBT ($\chi^{(3)}(-\omega;\omega,-\omega,\omega)$ being derived from degenerate four wave mixing).[11,12] The aligned solutions studied here afford the opportunity to elucidate certain of the components $|\chi^{(3)}|_{ijkl}$ of the susceptibility tensor. The PBT samples studied previously did not possess the alignment of the samples examined in this works. For an isotropic sample, third-harmonic measurements give the averaged value $|\chi^{(3)}|_{ISO} = \Sigma |\chi^{(3)}|_{ijij}/5$.[13]

Previous studies with the present nematic PBT solutions have shown them to be strongly birefringent, with a birefringence Δn that increases essentially linearly with the the polymer volume fraction.[14] This property was successfully exploited to extract a value for the order parameter: $S = 0.94$. Such a value reflects the very high alignment of the polymer rods in the present solutions.[14] The refractive index measurements show that both the extraordinary and the ordinary refractive indices, n_E and n_O, respectively, depend on the wavelength λ, with (X is E or O)

$$\frac{(n_X^2 - 1)}{(n_X^2 + 2)} = K\frac{\lambda^2}{\lambda^2 - \lambda_x^2} \tag{2}$$

where λ_E and λ_O were found to be 250 and 200 nm, respectively, and K was 0.27 for both n_E and n_O.[14] Analysis of the experimental results obtained here makes use of these refractive indices.

EXPERIMENTAL

Materials: The PBT (M_w = 34,000) was provided by SRI International. The polymer was dried in vacuum and dissolved in distilled, anhydrous methane sulfonic acid (MSA) using procedures discussed elsewhere.[9] Dissolution in MSA is accompanied by protonation of the solute macromolecules.[9] Solutions of PBT are nematic when formed with a volume fraction φ above a critical value ϕ_{NI}, where ϕ_{NI} depends on the chain length and the temperature: ϕ_{NI} = 0.03 for the PBT used at 25°C. The alignment procedure, described elsewhere,[14,15] consists of a surface alignment preparation using a suitable flow in a rectangular channel, followed by imposition of an external magnetic field (5 to 7 Tesla) in the sample plane, and along the flow direction, to speed the bulk alignment. With suitable surface alignment, the nematic monodomains are stabilized for an indefinite duration.

Nonlinear Optical Measurements: Third harmonic generation (THG) technique has been used to determine the third-order susceptibility.[1,2,11] The THG apparatus utilizes a Raman Cell filled with methane gas to provide a fundamental intensity I_ω at wavelength λ = 1542 nm, when pumped at λ = 1064 nm by a pulsed Nd:YAG laser, generating third harmonic intensity $I_{3\omega}$ at λ = 514 nm. The Maker Fringe Pattern (MFP), generated by $I_{3\omega}$ and used to study the third-order susceptibility, may be formed on rotation of a plane parallel sample, or translation of a wedge-shaped sample, in an incident beam I_ω.[2,3,7] The incident beam is split into two beams, directed to the sample and the reference to account for fluctuations in the incident intensity. A weakly focused beam generates a sufficiently intense signal for accurate detection with the samples of interest here. A Fresnel Rhomb in the incident beam permits control of the incident polarization, and an analyzer in the THG beam allows selection of the polarization of the output signal.

Experiments used plane parallel cells, provided by Hellma Cells Inc. The cell walls were specified to $\lambda/4$ surface flatness; the

sample thickness L was 375 μm. The reduced intensity R(θ.L) is given by

$$R(\theta,L) = \frac{I_{3\omega}(\theta,L)_{SAMP}}{I_{3\omega}(0,L)_{REFR}} \tag{3}$$

where SAMP and REFR stand for the sample and reference, respectively, and θ is the incidence angle and L the physical thickness; θ is varied by rotation of the sample (fixed L) in the use of a parallel slab, and L is varied by translation of the sample (fixed θ, essentially equal to zero) in the use of a wedge-shaped sample.[2] A fused silica plate (L = 1.00 mm) was used as the reference.

The MFP exhibits damped and symmetric oscillations about θ = 0 for the rotating parallel slab cell.[2b.c] A general expression for R(θ,L) for an isotropic material is given by:[1-4]

$$R(\theta,L) = K_R \left(\frac{[Q(\theta)W(\theta,L)]_{SAMP}}{[Q(0)W(0,L)]_{REFR}} \right)^2 \tag{4}$$

$$W(\theta,L) = \frac{|\chi^{(3)}|_{EFF}}{|n_{3\omega}{}^2 - n_\omega{}^2|} \Omega(\theta,L) \tag{5}$$

where $|\chi^{(3)}|_{EFF}$ is the effective component of $\chi^{(3)}$, e.g., see Eqn (1), Q(θ) is a weakly decreasing function of increasing angle, related in part to the Fresnel factors (Q(0) is unity),[2] K_R is the ratio between the incident beam directed to the sample and that directed to the reference, and n_ω and $n_{3\omega}$ are the refractive indices at the fundamental and the THG frequencies, respectively.[1-4]

The function Ω(θ,L) accounts for the interference effects between two waves, propagating with frequency 3ω and velocities $c/n_{3\omega}$ and c/n_ω, giving rise to the MFP. For the case with weak absorption, characterized by absorbances α_ω and $\alpha_{3\omega}$ for the incident and THG beams, respectively, Ω(θ,L) may be expressed as:[2]

$$\Omega^2(\theta,L) = 2b\left(\frac{a - b}{2b} + \sin^2[\psi(\theta,L)]\right) \tag{6a}$$

Here,

$$\psi(\theta,L) = \pi L/2L_c(\theta) \qquad\qquad (6b)$$

$$4a = \exp(-\alpha_{3\omega}) + \exp(-2\alpha_\omega) \qquad\qquad (6c)$$

$$2b = \exp(-\alpha_{3\omega}/2)\exp(-\alpha_\omega) \qquad\qquad (6d)$$

where $\alpha = \mu L/\cos\theta'$, with μ the extinction coefficient, and the coherence length $L_c(\theta)$ may be expressed as

$$L_c(\theta) = \lambda/6|n_{3\omega}\cos(\theta'_{3\omega})-n_\omega\cos(\theta'_\omega)| \qquad\qquad (7)$$

with $L_c(0) = \lambda/6|n_{3\omega}-n_\omega|$; the primes denote propagation angles measured in the sample, related to angles in air through Snell's law, using the appropriate refractive index, see below. The effect of weak focusing of the incident beam is neglected as too small to be important under the conditions used.[2] In practice, the parameter K_R is evaluated by determination of $R_{STD}(0)$ for the response to a standard with known $|\chi^{(3)}|_{EFF}$, $n_{3\omega}$, n_ω, and thickness L. A BK7 plate (L = 3.00 mm) was used as the standard in the cited study. It should be noted that, for a finite $L_c(0)$, R(0,L) may take on any value from zero to its value R_{MAX}, as $\psi(\theta,L)$ is not usually equal to an odd multiple of $\pi/2$ at $\theta=0$. However, $\sin\psi$ may be taken as unity for the successive maxima in the fringe pattern, providing a method to estimate of $|\chi^{(3)}|_{EFF}/|n_{3\omega}^2 - n_\omega^2|$ from data on R(θ,L). We have also shown, in previous measurements, that the THG analyzed here is mainly generated from the solute polymer. The contribution from the solvent and the cell walls are negligible: less than 5% for solutions with volume fraction $\varphi = 0.02 - 0.055$.[10]

For an anisotropic material, the parameter $|\chi^{(3)}|_{EFF}$ becomes the modulus of an appropriate component of the tensor $\chi^{(3)}$, depending on the polarization of the light and the orientation of the director n. In addition, the birefringence expected with an anisotropic material may modify the MFP, see below.
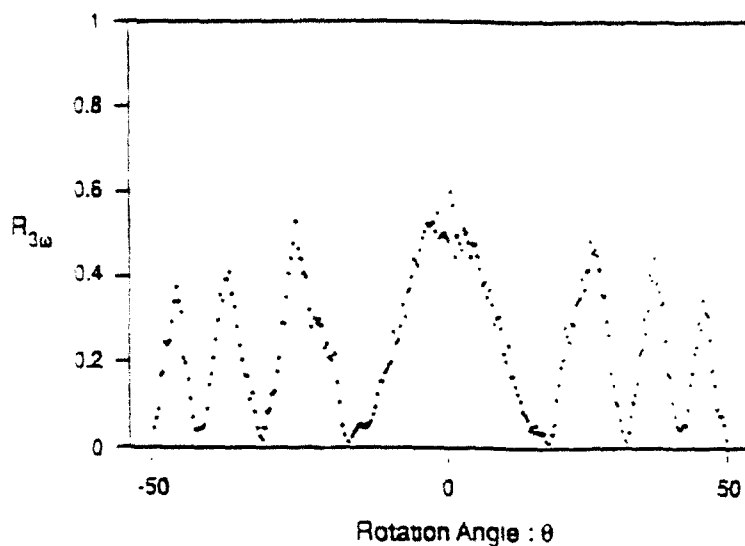
FIGURE 1   Maker Fringe Patterns for a nematic solution of PBT, with parallel polars and the incident polarization orthogonal to the director (e.g., arrangement V-h-V or H-v-H).

RESULTS

With nematic solutions, the response $R(\theta,L)$ depends on the polarizations of the incident light and the detected THG signal, and the orientation of these relative to the sample director (the preferred optical axis). Several geometric arrangements are of interest, depending on the relative orientations of the polarizations of the incident and THG fields, E_{INC} and E_{THG}, respectively, and the director n of the monodomain with respect to the axis of rotation; the latter was always vertical in the arrangements used. For convenience, the dependence of $R(\theta,L)$ on L is suppressed hereafter. All data were obtained using 1542 nm incident wavelength. The large birefringence of the PBT monodomain complicates the analysis is some cases, as the relevant refractive index varies with θ for certain arrangements, see below. In the following, the notation gives the orientations of these fields in the order $E_{THG}:n:E_{INC}$, e.g., V-h-H signifies an arrangement with E_{THG} vertical (parallel to the rotation axis) and both E_{INC} and n horizontal.
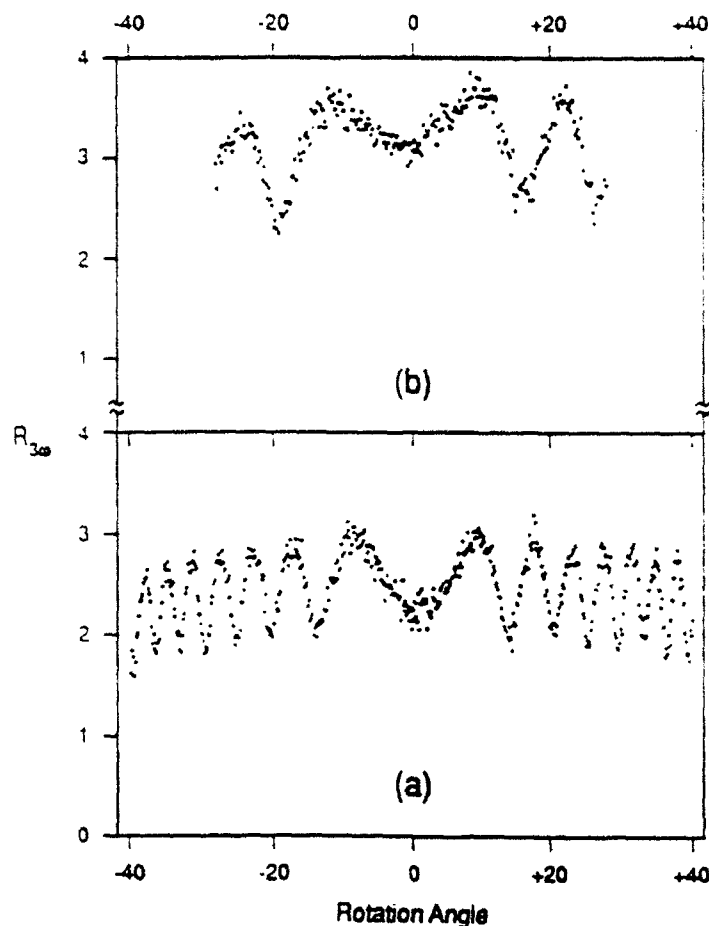
FIGURE 2   Maker Fringe Patterns for a nematic solution of PBT, with parallel polars and the incident polarization parallel to the director arrangement V-v-V (a) and H-h-H (b).

As may be seen in the preceding, it is necessary to know $n_{3\omega}$ and n_ω to determine $|\chi^{(3)}|_{EFF}$ from $R(\theta)$.

As shown in Fig. 1, the MFP for $R_{VhV}(\theta)$ and $R_{HvH}(\theta)$ were equivalent (except for small difference in amplitude due to the Fresnel factors), as expected, since all rays propagate with refractive index n_O. The analysis using the measured refractive indices gave $|\chi^{(3)}|_{VhV}/\varphi = |\chi^{(3)}|_{HvH}/\varphi$ with results given in Table I. The value is smaller than $|\chi^{(3)}|_{ISO}/\varphi$, as expected if the components to $\chi^{(3)}$ along the chain axis exceed those orthogonal to that axis. In component notation, $|\chi^{(3)}|_{VhV}$ and $|\chi^{(3)}|_{HvH}$ both correspond to
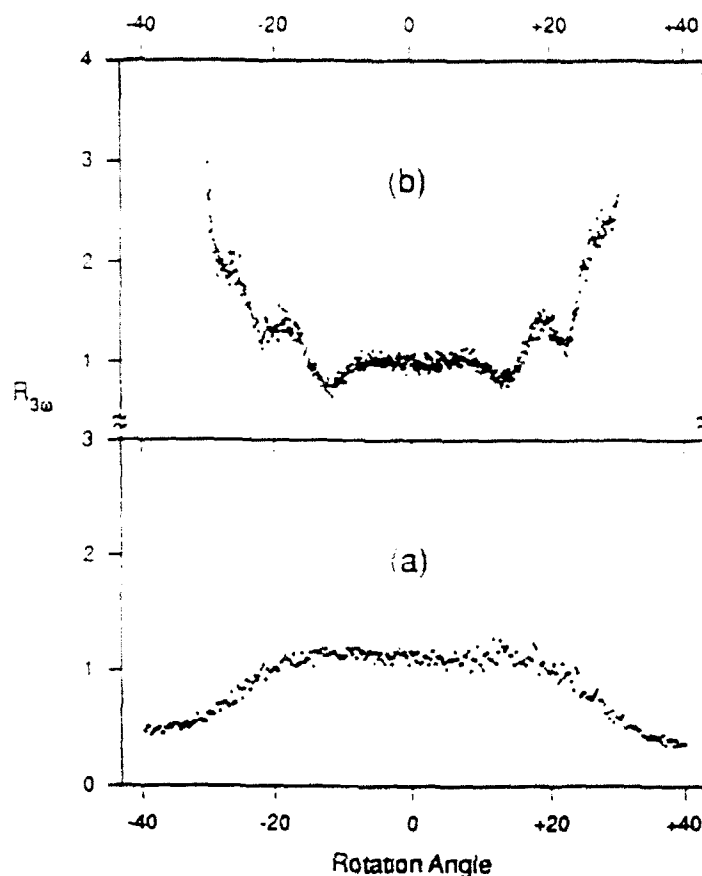
FIGURE 3   Maker Fringe Patterns for a nematic solution of PBT. with crossed polars and the incident polarization parallel to the director arrangement H-v-V (a) and V-h-H (b).

$|\chi^{(3)}|_{yyyy}$ with the x and z Cartesian coordinates along the director and orthogonal to the sample plane, respectively.

The depolarized signals $R_{Hhv}(\theta)$ and $R_{VvH}(\theta)$ were both nil ($R(\theta)$ < 0.01), showing that the signals $R_{HvH}(\theta)$ and $R_{Vhv}(\theta)$ discussed above are plane polarized.   In the component notation used above, $|\chi^{(3)}|_{Hhv}$ and $|\chi^{(3)}|_{VvH}$ both correspond to $|\chi^{(3)}|_{xyyy}$.

As shown in Figs. 2 and 3. the behavior is more complex for data on $R_{Vvv}(\theta)$, $R_{HhH}(\theta)$. $R_{Hvv}(\theta)$ and $R_{VhH}(\theta)$:   the minima are observed to be nonzero in all cases, and for $R_{Hvv}(\theta)$. only one broad peak is observed.   Separate experiments showed that no fluorescence contribution, caused by absorption at $\lambda_{3\omega} = 514$ nm, was observed for a scan of λ from 532 to 800 nm, permitting

TABLE I Third- order susceptibilities for PBT

x-axis along the cell axis
(the director for nematic sample)

P_i	$E_{j,k,l}$	COMPONENT	χ_{ijjl} ($\times 10^{-9}$ esu)
		ISOTROPIC SAMPLE:	$\rho = 0.02$
x(y)	x(y)	Polarized	(20)
x(y)	y(x)	Depolarized	(6)
		NEMATIC SAMPLE:	$\rho = 0.055$
x	x	xxxx	640
y	y	yyyy	
y	x	yxxx	
x	y	xyyy	(1)

ϕ is the PBT volume fraction

elimination of this factor as the cause of the nonzero minima.
Although the nonzero minima are reminiscent of the behavior
noted for an isotropic sample of PBT in MSA at incident wavelength
of 1907 nm, such behavior was not observed with the latter for
1542 nm incident wavelength, and calculations using Eqn (6) and
the experimental values for $\alpha_{3\omega}$ and α_ω show that that is not the
source of the behavior observed here. The nonzero $R_{HVV}(\theta)$
observed demonstrates that $\chi^{(3)}$ must have a nonzero χ yxxx
component in the coordinate system used here, but as discussed
below, the evaluation of that component may be compromised by
the birefringent nature of the material. A manifestation of the
component off the director axis is seen when the intensity (ratio)
$R_\beta(0,L)$ is determined with vertical director and incident light
polarized at angle β to the director (no analyzer) is studied: the
maximum in $R_\beta(0,L)$ occurs with the $\beta = +$ or $- 40$ degrees for the
present monodomain. This result will be discussed subsequently.[16]

Part of the behavior is clearly related to the refractive index
for the propagating beams in the birefringent material. Thus, for
$R_{VV}(\theta)$, the incident beam propagates with refractive index n_E for
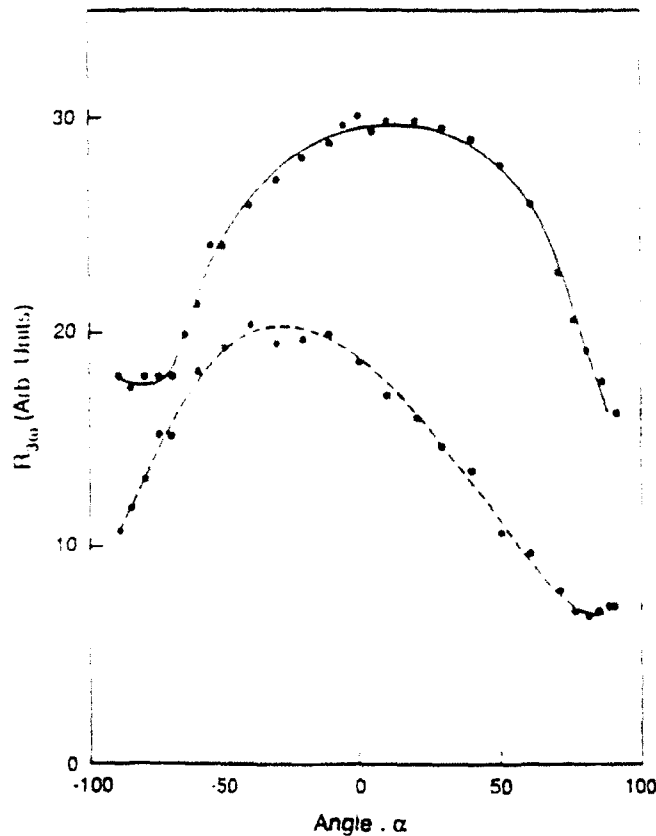
FIGURE 4 The parameter $R_O(0,L)$ determined with vertical director, vertically polarized incident light and analyzer at angle α to the polarizer for sample thickness L=385 μm (top curve), and L=438μm (bottom curve).

all θ, but for $R_{HhH}(\theta)$, the incident beam propagates with refractive index $n_e(\theta)$, where

$$n_e(\theta) = \left\{ \left(\frac{\cos\theta}{n_E}\right)^2 + \left(\frac{\sin\theta}{n_O}\right)^2 \right\}^{-1/2} \tag{8}$$

This accounts for part of the difference in the MFP seen for $R_{VvV}(\theta)$ and $R_{HhH}(\theta)$; the difference in the amplitudes of $R_{VvV}(0)$ and $R_{HhH}(0)$ noted in Fig. 3 reflects variation in K_R, and is removed in the final analysis. In addition, the appearance of the MFP for $R_{HvV}(\theta)$ and $R_{VhH}(\theta)$ is due in part to the materials high birefringence. For example, consideration of the values of $n_{E,\omega}$ and $n_{O,3\omega}$ shows that

these are so nearly similar that $\psi(\theta) < \pi$ for the available range in θ. resulting in the broad peak observed for $R_{HVV}(\theta)$ (Fig. 3a). The increasing $R_{VhH}(\theta)$ noted with increasing θ is caused by the decreasing difference between $n_{e,\omega}(\theta)$ and $n_{O,3\omega}$ with increasing θ (Fig. 3b). In addition to these considerations. a THG beam created with polarization neither parallel nor orthogonal to the director will propagate as two beams. one each polarized in these directions in the birefringent sample. and propagating with distinct refractive indices that may depend on θ, producing elliptically polarized beam. For the observed THG signal. e.g., the nematic slab is a retarder. This can result in the nonzero minima noted in Figs. 2 and 3. A manifestation of this is observed in $R_\alpha(0,L)$ determined with vertical director and vertically polarized incident light, and an analyzer at angle α to the polarizer. The maximum in $R_\alpha(0,L)$ occurs with angle α_m that depends on the sample thickness L as shown in Fig. 4. The difference in intensity between the two cases is due to the dependence of the function $\Omega(0,L)$ on the thickness (Eqns. (5) and (6)).

In order to proceed, apparent values of $|\chi^{(3)}|_{VVV}$, $|\chi^{(3)}|_{HhH}$, $|\chi^{(3)}|_{VhH}$, and $|\chi^{(3)}|_{HVV}$ can be deduced from $R_{VVV}(0)$, $R_{HhH}(0)$, $R_{VhH}(0)$. and $R_{HVV}(0)$, respectively, using the relevant refractive indices. These are entered in Table I. With neglect of the complications from the birefringence. $|\chi^{(3)}|_{VVV}$ and $|\chi^{(3)}|_{HhH}$, would both correspond to $|\chi^{(3)}|_{xxxx}$, and $|\chi^{(3)}|_{VhH}$ and $|\chi^{(3)}|_{HVV}$ would correspond to $|\chi^{(3)}|_{yxxx}$. Owing to the birefringent nature of the material. the numerical values reported in Table I for these parameters may be suspect. but it seems unlikely that their general ranking will be altered if the birefringence is taken into account.

DISCUSSION

Summarizing the results, in component notation, $|\chi^{(3)}|_{xxxx} \gg |\chi^{(3)}|_{yyyy} > |\chi^{(3)}|_{yxxx} > |\chi^{(3)}|_{xyyy}$, but $|\chi^{(3)}|_{xxxx}$ is not the largest projection of $\chi^{(3)}$. By comparison with the data in Table I. $|\chi^{(3)}|_{iso}/\varphi$ determined for isotropic solutions of PBT in MSA is given in Table I

for comparison.[10] Of course, the principal interest here is not only in the $|\chi^{(3)}|_{ijkl}$ but in the corresponding components $|\gamma|_{ijkl}$ of the second hyperpolarizability tensor γ. In general, a relation between $\chi^{(3)}$ and γ may be written as:[2,3]

$$\chi^{(3)}(-\omega; \omega_1,\omega_2,\omega_3) = f(\omega)f(\omega_1)f(\omega_2)f(\omega_3)N\gamma(-\omega; \omega_1,\omega_2,\omega_3) \qquad (11)$$

where the $f(\omega_i)$ are local field factors and N is the number of molecules per unit volume. An eventual goal is to be able to reliably estimate $\gamma(-\omega; \omega_1,\omega_2,\omega_3)$ from information on the molecular structure, and to maximize the desired response by manipulation of the latter. The behavior reported here indicates that the maximum component to γ is off the molecular axis, contrary to what one might have anticipated.[6,16,17] This behavior requires that a relevant electronic transition in the NLO response of the solvated PBT is at an appreciable angle to the chain axis. This is distinctly different from the result of calculations on conjugated *cis* and *trans* polyenes, for which it is predicted that the principal component to γ will have all electromagnetic fields polarized along the molecular axis.[17] With PBT, a possible candidate for a vector associated with an electronic transition off axis to the rodlike molecular axis is the vector along the sulfur-sulfur atoms in the repeating unit of the chain. This possibility opens the question of whether γ for PBT is influenced by the polymeric rodlike character of the molecule, or whether γ would be essentially the same for a short oligomeric PBT as for a long-chain molecule, perhaps even a model of the repeat unit (i.e., the repeat unit terminated by protons).

REFERENCES

1. *Nonlinear Optical Properties of Organic Molecules and Crystals*, Ed. by S. Chemla, J. Zyss, Academic Press, Vol. 1 and 2 (1987).

2. a) Y. R. Shen, *The Principle of Nonlinear Optics*, J. Wiley, New York (1984).
    b) S. K. Kurtz, in *Quantum Electronics*, Ed. by H. Rabin and C. L. Tang, Vol. 1, Part A, Academic Press, N.Y. (1975), Chapt. 3 and references therein.
    c) F. Kajzar, J. Messier, *Phys. Rev. A*, 32, 2353 (1985).
3. A. Yariv, *Quantum Electronics*, J. Wiley, New York (1989).
4. *Nonlinear Optical Properties of Polymers*, Ed. by A. J. Heeger, J. Orenstein, D. R. Ulrich, Matl. Res. Soc. Symp. Proceed. Vol. 109 (1988).
5. *Optical and Electrical Properties of Polymers*, Ed. by J. M. Torkelson and J. A. Emerson, Matl. Res. Soc. Symp. Proceed. Vol. 214 (1991).
6. P. N. Prasad, D. J. Williams, *Introduction to Nonlinear Optical Effects in Molecules and Polymers*, J. Wiley, New York, 1991.
7. J. Zyss, D. S. Chemla, Chapt. II-1 in ref. 1.
8. F. Kajzar, J. Messier, Chapt. III-2 in ref. 1.
9. a) G. C. Berry, P. R. Eisaman, *J. Polym. Sci., Polym. Phys. Ed.* 12:2253 (1974).
    b) C. C. Lee, S. G. Chu, G. C. Berry, *J. Polym. Sci., Polym. Phys. Ed.* 21:1573 (1983).
10. a) H. Mattoussi, P. G. Kaatz, G. D. Patterson, G. C. Berry, in ref. 5, p. 11.
    b) H. Mattoussi, G. C. Berry, *ACS Polym. Preprints* 32(3): 690 (1991).
11. H. Vanherzeele, J. S. Meth, S. A. Jenekhe, M. F. Roberts, *Appl. Phys. Lett.* 58: 663 (1991).
12. D. N. Rao, J. Swiatkiewicz, P. Chopra, S. K. Choshal, P. N. Prasad, *Appl. Phys. Lett.* 48: 1187 (1986).
13. D. Pugh, J. O. Morley, Chapt. II-2 in ref. 1.
14. a) H. Mattoussi, M. Srinivasarao, P. G. Kaatz, G. C. Berry, in ref. 5, p. 157; and in this proceeding.
    b) H. Mattoussi, M. Srinivasarao, P. G. Kaatz, G. C. Berry, *Macromolecules*, in press.
15 G. C. Berry, *Disc. Faraday Soc.* No. 79, 141 (1985).
16 H. Mattoussi, G. C. Berry, in preparation.
17 A. F. Garito, C. C. Teng, *Proc. Soc. Photo-Opt. Instrum. Eng.* 613: 146 (1986).